Available online at www.sciencedirect.com
ScienceDirect
Journal of Sound and Vibration 319 (2009) 593–605
JOURNAL OF SOUND AND VIBRATION
www.elsevier.com/locate/jsvi

On the natural frequencies and mode shapes of a multispan Timoshenko beam carrying a number of various concentrated elements

Hsien-Yuan Lin*

Department of Mechanical Engineering, Cheng Shiu University, 840, Chengcing Road, Niaosong Township, Kaohsiung County 83347, Taiwan, Republic of China

Received 29 January 2008; received in revised form 12 May 2008; accepted 16 May 2008
Handling Editor: L.G. Tham
Available online 7 July 2008

Abstract

The purpose of this paper is to utilize the numerical assembly method (NAM) to determine the exact natural frequencies and mode shapes of the multispan Timoshenko beam carrying a number of various concentrated elements including point masses, rotary inertias, linear springs, rotational springs and spring–mass systems. First, the coefficient matrices for an intermediate pinned support, an intermediate concentrated element, left- and right-end support of a Timoshenko beam are derived. Next, the overall coefficient matrix for the whole structural system is obtained using the numerical assembly technique of the finite element method. Finally, the exact natural frequencies and the associated mode shapes of the vibrating system are determined by equating the determinant of the last overall coefficient matrix to zero and substituting the corresponding values of integration constants into the associated eigenfunctions, respectively. The effects of distribution of in-span pinned supports and various concentrated elements on the dynamic characteristics of the Timoshenko beam are also studied.

1. Introduction

A beam being short in length relative to its transverse dimensions or a long beam vibrating in a higher mode so that the nodal points are close together, a deformation due to the shear stress occurs in the beam except that it is subjected only to the pure bending moment. In such situation, it is necessary to use the full Timoshenko theory of beam deformation. Many researchers [1–4] studied the vibration problems of a cantilever Timoshenko beam with a tip body at its free end. Maurizi and Bellés [5] studied the natural frequencies of the beam–mass system of a simply supported uniform Timoshenko beam. Abramovich and Hamburger [6] studied the vibration of a uniform cantilever Timoshenko beam with translational and rotational springs and with a tip mass. Rossi et al. [7] studied the free vibration of Timoshenko beams carrying elastically mounted, concentrated masses. Posiadala [8] studied the free vibrations of uniform Timoshenko beams with attachments

*Tel.: +886 7 3496561; fax: +886 7 3371000.
E-mail addresses: linsyg@csu.edu.tw, lin.syg@msa.hinet.net.

0022-460X/$ - see front matter © 2008 Elsevier Ltd. All rights reserved.
doi:10.1016/j.jsv.2008.05.022

Nomenclature

A	cross-sectional area of the beam
E	Young's modulus of the beam
G	shear modulus of the beam
I	moment of inertia of cross-sectional area A of the beam
j	$\sqrt{-1}$
J_v	rotary inertia of lumped mass m_v at the vth station
k'	shear coefficient
k_{Rv}	rotational spring constant at the vth station
k_{Tv}	translational (linear) spring constant at the vth station
k_{eu}	spring constant of the spring–mass system at the uth station
L	total length of the beam
$\overline{m}$	mass per unit length of the beam
m_v	lumped mass at the vth station
m_{eu}	lumped mass of the spring–mass system at the uth station
n	total number of intermediate stations
q	total number of equations for the integration constants
$\overline{r}$	total number of intermediate pinned supports
R_g	radius of gyration of cross-sectional area A($R_g = \sqrt{I/A}$)
$\overline{u}$	total number of intermediate spring–mass systems
$\overline{v}$	total number of intermediate concentrated elements
x_u	axial coordinate of station u
$y(x, t)$	transverse displacement at position x and time t for the beam
$\overline{Y}$	amplitude function of $y(x, t)$
$z_u(t)$	instantaneous displacement for lumped mass m_{eu} of the spring–mass system at the uth station (relative to its static equilibrium position)
$\ddot{z}_u$	acceleration of $z_u(t)$
$\overline{Z}_u$	amplitude of $z_u(t)$
ρ	mass density of the beam
$\varphi(x, t)$	bending slope at position x and time t
ω_{eu}	natural frequency of the spring–mass system at the uth station (with respect to the static beam)
ω_{Ti}	ith natural frequency of Timoshenko beam
ω_{Ei}	ith natural frequency of Euler–Bernoulli beam
Ω_i	dimensionless frequency parameter corresponding to the ith vibration mode

by means of the Lagrange multiplier approach. Hong and Kim [9] proposed an exact modal analysis of multispan beam-type structure supported and/or connected by resilient joints with damping by means of the spatial domain Laplace transform. Gürgöze [10–12] presented the eigenfrequencies of a cantilever beam with attached tip mass and a spring–mass system and those of a cantilever beam with several spring–mass systems. Wu and Chen [13] presented a modified lumped-mass transfer matrix method for the free vibration analysis of a multistep Timoshenko beam carrying eccentric lumped masses with eccentricity and rotary inertias. Wu and Chen [14] obtained the exact solution of a single-span uniform Timoshenko beam carrying any number of spring–mass systems by using NAM. Lin and Tsai determined the exact values of natural frequencies and associated mode shapes of a "multispan" uniform beam carrying multiple spring–mass systems [15] and those of a multiple-step beam carrying a number of intermediate lumped masses and rotary inertias [16] with the NAM. From the foregoing literature review, one finds that the literature regarding determination of exact natural frequencies and mode shapes of a "multispan" Timoshenko beam carrying multiple various concentrated elements is little. Therefore, the objective of this paper is to extend the theory of NAM to investigate the free vibration characteristics of a multispan Timoshenko beam carrying multiple point masses, rotary inertias, linear springs, rotational springs and spring–mass systems.

2. Equation of motion and displacement function

Fig. 1 shows the sketch of a uniform beam supported by $\overline{r}$ pins, carrying $\overline{u}$ spring–mass systems and $\overline{v}$ various concentrated elements. If each of the points that the $\overline{r}$ intermediate pinned supports, the $\overline{u}$ spring–mass

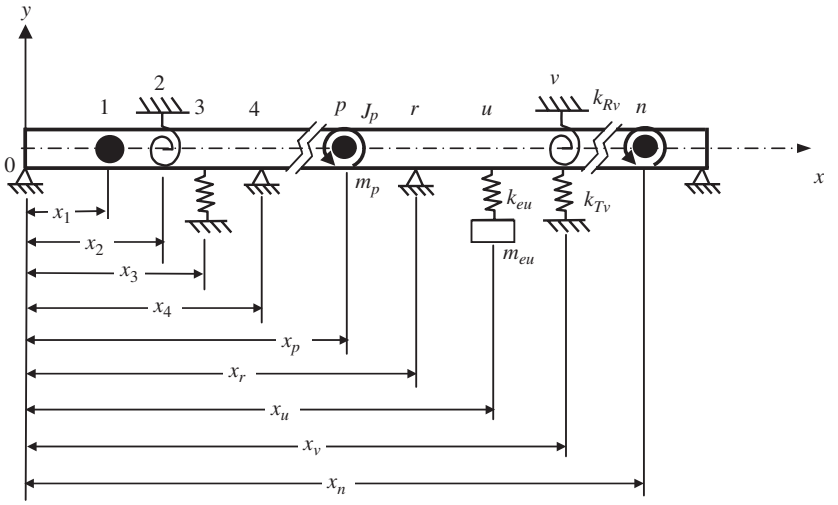

Fig. 1. Sketch for a uniform Timoshenko beam supported by $\overline{r}$ intermediate pins, carrying $\overline{u}$ spring–mass systems and $\overline{v}$ various concentrated elements.

systems or the $\overline{v}$ concentrated elements located is called a "station," then the total number of intermediate stations is n.

Considering the effects of shear deformation and rotary inertia, the equation of motion for a uniform beam is given by [17]

$$EI\frac{\partial^2\varphi(x,t)}{\partial x^2}+k'GA\left(\frac{\partial y(x,t)}{\partial x}-\varphi(x,t)\right)-R_g^2\overline{m}\frac{\partial^2\varphi(x,t)}{\partial^2 t}=0 \tag{1}$$

$$\overline{m}\frac{\partial^2 y(x,t)}{\partial t^2}-k'AG\left(\frac{\partial^2 y(x,t)}{\partial x^2}-\frac{\partial\varphi(x,t)}{\partial x}\right)=0 \tag{2}$$

where E is Young's modulus, A is the cross-sectional area, I is the moment of inertia of the cross-sectional area A about the axis of bending, k' is the shear coefficient, G is the shear modulus and ρ is the mass density of the beam material, $\overline{m}=\rho A$ is mass per unit length of the beam, $R_g=\sqrt{I/A}$ is radius of gyration of cross-sectional area A, $y(x, t)$ is the transverse deflection of the beam at position x and time t and $\varphi(x, t)$ is the bending slope.

Eqs. (1) and (2) are referred to as the Timoshenko beam equations and can be decoupled as follows:

$$EI\frac{\partial^4 y(x,t)}{\partial x^4}+\overline{m}\frac{\partial^2 y(x,t)}{\partial^2 t}-\overline{m}R_g^2\left(1+\frac{E}{k'G}\right)\frac{\partial^4 y(x,t)}{\partial^2 x\partial^2 t}+\left(\frac{\overline{m}^2R_g^2}{k'AG}\right)\frac{\partial^4 y(x,t)}{\partial t^4}=0 \tag{3}$$

$$EI\frac{\partial^4\varphi(x,t)}{\partial x^4}+\overline{m}\frac{\partial^2\varphi(x,t)}{\partial^2 t}-\overline{m}R_g^2\left(1+\frac{E}{k'G}\right)\frac{\partial^4\varphi(x,t)}{\partial^2 x\partial^2 t}+\left(\frac{\overline{m}^2R_g^2}{k'AG}\right)\frac{\partial^4\varphi(x,t)}{\partial t^4}=0 \tag{4}$$

Free vibration of the beam takes the form

$$y(x,t)=\overline{Y}(x)\,e^{j\omega t} \tag{5}$$

$$\varphi(x,t)=\overline{\Psi}(x)\,e^{j\omega t} \tag{6}$$

where $\overline{Y}(x)$ and $\overline{\Psi}(x)$ are the amplitude functions of $y(x, t)$ and $\varphi(x, t)$, respectively, ω is natural frequency of the whole vibrating system and $j=\sqrt{-1}$.

Substituting Eqs. (5) and (6) into Eqs. (3) and (4), respectively, one obtains

$$\overline{Y}'''' + (a+b)\overline{Y}'' - (c-ab)\overline{Y} = 0 \tag{7}$$

$$\overline{\Psi}'''' + (a+b)\overline{\Psi}'' - (c-ab)\overline{Y} = 0 \tag{8}$$

where

$$a = \frac{\overline{m}\omega^2}{k'AG}, \quad b = \frac{\rho I\omega^2}{EI}, \quad c = \frac{\overline{m}\omega^2}{EI} \tag{9a–c}$$

The general solutions of Eqs. (7) and (8) take the forms

$$\overline{Y}(x) = C_1 \sin(\lambda_1 x) + C_2 \cos(\lambda_1 x) + C_3 \sinh(\lambda_2 x) + C_4 \cosh(\lambda_2 x) \tag{10}$$

$$\overline{\Psi}(x) = C'_1 \sin(\lambda_1 x) + C'_2 \cos(\lambda_1 x) + C'_3 \sinh(\lambda_2 x) + C'_4 \cosh(\lambda_2 x) \tag{11}$$

where C_p and C'_p ($p = 1, 2, 3, 4$) are the integration constants, and

$$\lambda_1 = \left\{\tfrac{1}{2}[4c + (a-b)^2]^{1/2} + \tfrac{1}{2}(a+b)\right\}^{1/2} \tag{12a}$$

$$\lambda_2 = \left\{\tfrac{1}{2}[4c + (a-b)^2]^{1/2} - \tfrac{1}{2}(a+b)\right\}^{1/2} \tag{12b}$$

The substitution of Eqs. (5), (6), (10) and (11) into Eq. (1) gives

$$\begin{aligned}&\left(1 - \frac{\rho I\omega^2}{k'AG}\right)[C'_1 \sin(\lambda_1 x) + C'_2 \cos(\lambda_1 x) + C'_3 \sinh(\lambda_2 x) + C'_4 \cosh(\lambda_2 x)]\\ &- \frac{EI}{k'AG}[-C'_1\lambda_1^2 \sin(\lambda_1 x) - C'_2\lambda_1^2 \cos(\lambda_1 x) + C'_3\lambda_2^2 \sinh(\lambda_2 x) + C'_4\lambda_2^2 \cosh(\lambda_2 x)]\\ &= C_1\lambda_1 \cos(\lambda_1 x) - C_2\lambda_1 \sin(\lambda_1 x) + C_3\lambda_2 \cosh(\lambda_2 x) + C_4\lambda_2 \sinh(\lambda_2 x)\end{aligned} \tag{13}$$

$$C'_1 = -\alpha_1 C_2, \quad C'_2 = \alpha_1 C_1, \quad C'_3 = \alpha_2 C_4, \quad C'_4 = \alpha_2 C_3 \tag{14a–d}$$

where

$$\alpha_1 = \frac{\lambda_1}{[1 - (\rho I\omega^2/k'AG)] + (EI/k'AG)\lambda_1^2}, \quad \alpha_2 = \frac{\lambda_2}{[1 - (\rho I\omega^2/k'AG)] - (EI/k'AG)\lambda_2^2} \tag{15a,b}$$

3. Determination of coefficient matrices for the stations located by pin supports, concentrated elements and beam ends

For an arbitrary station located at x_s (cf. Fig. 1), from Eqs. (10) and (11) one obtains

$$\overline{Y}_s(x_s) = C_{s,1} \sin(\lambda_1 x_s) + C_{s,2} \cos(\lambda_1 x_s) + C_{s,3} \sinh(\lambda_2 x_s) + C_{s,4} \cosh(\lambda_2 x_s) \tag{16}$$

$$\overline{\Psi}_s(x_s) = C_{s,1}\alpha_1 \cos(\lambda_1 x_s) - C_{s,2}\alpha_1 \sin(\lambda_1 x_s) + C_{s,3}\alpha_2 \cosh(\lambda_2 x_s) + C_{s,4}\alpha_2 \sinh(\lambda_2 x_s) \tag{17}$$

$$\overline{Y'}_s(x_s) = C_{s,1}\lambda_1 \cos(\lambda_1 x_s) - C_{s,2}\lambda_1 \sin(\lambda_1 x_s) + C_{s,3}\lambda_2 \cosh(\lambda_2 x_s) + C_{s,4}\lambda_2 \sinh(\lambda_2 x_s) \tag{18}$$

$$\overline{\Psi}'_s(x_s) = -C_{s,1}\alpha_1\lambda_1 \sin(\lambda_1 x_s) - C_{s,2}\alpha_1\lambda_1 \cos(\lambda_1 x_s) + C_{s,3}\alpha_2\lambda_2 \sinh(\lambda_2 x_s) + C_{s,4}\alpha_2\lambda_2 \cosh(\lambda_1 x_s) \tag{19}$$

where the primes refer to differentiation with respect to the coordinate x.

If the station numbering corresponding to the intermediate spring–mass system is represented by u, then the continuity of deformations and equilibrium of moments and forces require that

$$\overline{Y}_u^L(x_u) = \overline{Y}_u^R(x_u) \tag{20}$$

$$\overline{\Psi}_u^L(x_u) = \overline{\Psi}_u^R(x_u) \tag{21}$$

$$\overline{\Psi}'^L_u(x_u) = \overline{\Psi}'^R_u(x_u) \tag{22}$$

$$k'AG[\overline{\Psi}_u^L(x_u) - \overline{Y}'^L_u(x_u)] + F_u^*\overline{Y}(x_u) = k'AG[\overline{\Psi}_u^R(x_u) - \overline{Y}'^R_u(x_u)] \tag{23}$$

$$F_u^* = \frac{m_{eu}\omega^2}{1-(\omega/\omega_{eu})^2} \tag{24}$$

In Eqs. (20)–(23), the superscripts "L" and "R" refer to the left-hand and right-hand side of station u, respectively.

The equation of motion for the intermediate spring–mass system of uth station is given by

$$m_{eu}\ddot{z}_u + k_{eu}(z_u - y_u) = 0 \tag{25}$$

Free vibration of the spring–mass system takes the form

$$z_u(t) = \overline{Z}_u\, e^{j\omega t} \tag{26}$$

with $\overline{Z}_u$ denoting the amplitude of $z(t)$, then the substitution of Eqs. (5) and (25) into Eq. (24) gives

$$\overline{Y}_u(x_u) + [(\omega/\omega_{eu})^2 - 1]\overline{Z}_u = 0 \tag{27}$$

$$\omega_{eu} = \left(\frac{k_{eu}}{m_{eu}}\right)^{1/2} \tag{28}$$

where m_{eu} and k_{eu} denote the point mass and spring constant of the spring–mass system of uth station, respectively, z_u and $\ddot{z}_u$ denote the displacement and acceleration of the spring mass (m_{eu}) relative to its static equilibrium position, and ω_{eu} defined by Eq. (28) denotes the natural frequency of the spring–mass system with respect to the static beam.

Substituting Eqs. (16)–(19) into Eqs. (20)–(23) and (27), respectively, one obtains

$$\begin{aligned} &C_{u,1}\sin(\lambda_1 x_u) + C_{u,2}\cos(\lambda_1 x_u) + C_{u,3}\sinh(\lambda_2 x_u) + C_{u,4}\cosh(\lambda_2 x_u) \\ &\quad - C_{u+1,1}\sin(\lambda_1 x_u) - C_{u+1,2}\cos(\lambda_1 x_u) - C_{u+1,3}\sinh(\lambda_2 x_u) - C_{u+1,4}\cosh(\lambda_2 x_u) = 0 \end{aligned} \tag{29}$$

$$\begin{aligned} &C_{u,1}\alpha_1\cos(\lambda_1 x_u) - C_{u,2}\alpha_1\sin(\lambda_1 x_u) + C_{u,3}\alpha_2\cosh(\lambda_2 x_u) + C_{u,4}\alpha_2\sinh(\lambda_2 x_u) \\ &\quad - C_{u+1,1}\alpha_1\cos(\lambda_1 x_u) + C_{u+1,2}\alpha_1\sin(\lambda_1 x_u) - C_{u+1,3}\alpha_2\cosh(\lambda_2 x_u) - C_{u+1,4}\alpha_2\sinh(\lambda_2 x_u) = 0 \end{aligned} \tag{30}$$

$$\begin{aligned} &-C_{u,1}\alpha_1\lambda_1\sin(\lambda_1 x_u) - C_{u,2}\alpha_1\lambda_1\cos(\lambda_1 x_u) + C_{u,3}\alpha_2\lambda_2\sinh(\lambda_2 x_u) + C_{u,4}\alpha_2\lambda_2\cosh(\lambda_2 x_u) \\ &+ C_{u+1,1}\alpha_1\lambda_1\sin(\lambda_1 x_u) + C_{u+1,2}\alpha_1\lambda_1\cos(\lambda_1 x_u) - C_{u+1,3}\alpha_2\lambda_2\sinh(\lambda_2 x_u) - C_{u+1,4}\alpha_2\lambda_2\cosh(\lambda_2 x_u) = 0 \end{aligned} \tag{31}$$

$$\begin{aligned} &k'AG[C_{u,1}\alpha_1\cos(\lambda_1 x_u) - C_{u,2}\alpha_1\sin(\lambda_1 x_u) + C_{u,3}\alpha_2\cosh(\lambda_2 x_u) + C_{u,4}\alpha_2\sinh(\lambda_2 x_u) \\ &\quad - C_{u,1}\lambda_1\cos(\lambda_1 x_u) + C_{u,2}\lambda_1\sin(\lambda_1 x_u) - C_{u,3}\lambda_2\cosh(\lambda_2 x_u) - C_{u,4}\lambda_2\sinh(\lambda_2 x_u)] \\ &\quad + F_u^*[C_{u,1}\sin(\lambda_1 x_u) + C_{u,2}\cos(\lambda_1 x_u) + C_{u,3}\sinh(\lambda_2 x_u) + C_{u,4}\cosh(\lambda_2 x_u)] \\ &\quad - k'AG[C_{u+1,1}\alpha_1\cos(\lambda_1 x_u) - C_{u+1,2}\alpha_1\sin(\lambda_1 x_u) + C_{u+1,3}\alpha_2\cosh(\lambda_2 x_u) + C_{u+1,4}\alpha_2\sinh(\lambda_2 x_u) \\ &\quad - C_{u+1,1}\lambda_1\cos(\lambda_1 x_u) + C_{u+1,2}\lambda_1\sin(\lambda_1 x_u) - C_{u+1,3}\lambda_2\cosh(\lambda_2 x_u) - C_{u+1,4}\lambda_2\sinh(\lambda_2 x_u)] = 0 \end{aligned} \tag{32}$$

$$C_{u,1}\sin(\lambda_1 x_u) + C_{u,2}\cos(\lambda_1 x_u) + C_{u,3}\sinh(\lambda_2 x_u) + C_{u,4}\cosh(\lambda_2 x_u) + [(\omega/\omega_{eu})^2 - 1]\overline{Z}_u = 0 \tag{33}$$

Writing Eqs. (29)–(33) in matrix form, one obtains

$$[B_u] \quad \{C_u\} = 0 \tag{34}$$

where

$$\{C_u\} = \left\{ C_{u,1} \quad C_{u,2} \quad C_{u,3} \quad C_{u,4} \quad C_{u+1,1} \quad C_{u+1,2} \quad C_{u+1,3} \quad C_{u+1,4} \quad \overline{Z}_u \right\} \tag{35}$$

and the coefficient matrix $[B_u]$ is given by Eq. (A.1) in Appendix A at the end of this paper. In Eq. (34), the symbols, [] and {}, denote the rectangular matrix and column vector, respectively.

If the station numbering corresponding to the intermediate concentrated elements (including point masses, rotary inertias, linear springs and rotational springs) is represented by v, then the continuity of deformations and equilibrium of moments and forces require that

$$\overline{Y}_v^L(x_v) = \overline{Y}_v^R(x_v) \tag{36}$$

$$\overline{\Psi}_v^L(x_v) = \overline{\Psi}_v^R(x_v) \tag{37}$$

$$EI\overline{\Psi}'^R_v(x_v) - (J_v\omega^2 - k_{Rv})\overline{\Psi}_v^L(x_v) = EI\overline{\Psi}'^R_v(x_v) \tag{38}$$

$$k'AG[\overline{\Psi}_v^L(x_v) - \overline{Y}'^L_v(x_v)] + (m_v\omega^2 - k_{Tv})\overline{Y}_v^L(x_v) = k'AG[\overline{\Psi}_v^R(x_v) - \overline{Y}'^R_v(x_v)] \tag{39}$$

Substituting Eqs. (16)–(19) into Eqs. (36)–(39), respectively, one obtains

$$\begin{aligned} &C_{v,1}\sin(\lambda_1 x_v) + C_{v,2}\cos(\lambda_1 x_v) + C_{v,3}\sinh(\lambda_2 x_v) + C_{v,4}\cosh(\lambda_2 x_v) \\ &\quad - C_{v+1,1}\sin(\lambda_1 x_v) - C_{u+1,2}\cos(\lambda_1 x_v) - C_{v+1,3}\sinh(\lambda_2 x_v) - C_{v+1,4}\cosh(\lambda_2 x_v) = 0 \end{aligned} \tag{40}$$

$$\begin{aligned} &C_{v,1}\alpha_1\cos(\lambda_1 x_v) - C_{v,2}\alpha_1\sin(\lambda_1 x_v) + C_{v,3}\alpha_2\cosh(\lambda_2 x_v) + C_{v,4}\alpha_2\sinh(\lambda_2 x_v) \\ &\quad - C_{v+1,1}\alpha_1\cos(\lambda_1 x_v) + C_{v+1,2}\alpha_1\sin(\lambda_1 x_v) - C_{v+1,3}\alpha_2\cosh(\lambda_2 x_v) - C_{v+1,4}\alpha_2\sinh(\lambda_2 x_v) = 0 \end{aligned} \tag{41}$$

$$\begin{aligned} &EI[-C_{v,1}\alpha_1\lambda_1\sin(\lambda_1 x_v) - C_{v,2}\alpha_1\lambda_1\cos(\lambda_1 x_v) + C_{v,3}\alpha_2\lambda_2\sinh(\lambda_2 x_v) + C_{v,4}\alpha_2\lambda_2\cosh(\lambda_2 x_v)] \\ &\quad - (J\omega^2 - k_{Rv})[C_{v,1}\alpha_1\lambda_1\cos(\lambda_1 x_v) - C_{v,2}\alpha_1\lambda_1\sin(\lambda_1 x_v) + C_{v,3}\alpha_2\lambda_2\cosh(\lambda_2 x_v) + C_{v,4}\alpha_2\lambda_2\sinh(\lambda_2 x_v)] \\ &\quad + EI[C_{v+1,1}\alpha_1\lambda_1\sin(\lambda_1 x_v) + C_{v+1,2}\alpha_1\lambda_1\cos(\lambda_1 x_v) - C_{v+1,3}\alpha_2\lambda_2\sinh(\lambda_2 x_v) - C_{v+1,4}\alpha_2\lambda_2\cosh(\lambda_2 x_v)] = 0 \end{aligned} \tag{42}$$

$$\begin{aligned} &k'AG[C_{v,1}\alpha_1\cos(\lambda_1 x_v) - C_{v,2}\alpha_1\sin(\lambda_1 x_v) + C_{v,3}\alpha_2\cosh(\lambda_2 x_v) + C_{v,4}\alpha_2\sinh(\lambda_2 x_v) \\ &\quad - C_{v,1}\lambda_1\cos(\lambda_1 x_v) + C_{v,2}\lambda_1\sin(\lambda_1 x_v) - C_{v,3}\lambda_2\cosh(\lambda_2 x_v) - C_{v,4}\lambda_2\sinh(\lambda_2 x_v)] \\ &\quad + (m_v\omega^2 - k_{Tv})[C_{v,1}\sin(\lambda_1 x_v) + C_{v,2}\cos(\lambda_1 x_v) + C_{v,3}\sinh(\lambda_2 x_v) + C_{v,4}\cosh(\lambda_2 x_v)] \\ &\quad - k'AG[C_{v+1,1}\alpha_1\cos(\lambda_1 x_v) - C_{v+1,2}\alpha_1\sin(\lambda_1 x_v) + C_{v+1,3}\alpha_2\cosh(\lambda_2 x_v) + C_{v+1,4}\alpha_2\sinh(\lambda_2 x_v) \\ &\quad - C_{v+1,1}\lambda_1\cos(\lambda_1 x_v) + C_{v+1,2}\lambda_1\sin(\lambda_1 x_v) - C_{v+1,3}\lambda_2\cosh(\lambda_2 x_v) - C_{v+1,4}\lambda_2\sinh(\lambda_2 x_v)] = 0 \end{aligned} \tag{43}$$

Writing Eqs. (41)–(43) in matrix form, one obtains

$$[B_v] \quad \{C_v\} = 0 \tag{44}$$

where

$$\{C_v\} = \left\{ C_{v,1} \quad C_{v,2} \quad C_{v,3} \quad C_{v,4} \quad C_{v+1,1} \quad C_{v+1,2} \quad C_{v+1,3} \quad C_{v+1,4} \right\} \tag{45}$$

and the coefficient matrix $[B_v]$ is given by Eq. (A.3) in Appendix A at the end of this paper.

Similarly, if the station numbering corresponding to the intermediate pinned–support is represented by r, then the continuity of deformations and equilibrium of moments require that

$$\overline{Y}_r^L(x_r) = \overline{Y}_r^R(x_r) = 0 \tag{46,47}$$

$$\overline{\Psi}_r^L(x_r) = \overline{\Psi}_r^R(x_r) \tag{48}$$

$$\overline{\Psi}'^L_r(x_r) = \overline{\Psi}'^R_r(x_r) \tag{49}$$

Substituting Eqs. (16)–(19) into Eqs. (46)–(49), respectively, one obtains

$$C_{r,1}\sin(\lambda_1 x_r)+C_{r,2}\cos(\lambda_1 x_r)+C_{r,3}\sinh(\lambda_2 x_r)+C_{r,4}\cosh(\lambda_2 x_r)=0 \tag{50}$$

$$C_{r+1,1}\sin(\lambda_1 x_r)+C_{r+1,2}\cos(\lambda_1 x_r)+C_{r+1,3}\sinh(\lambda_2 x_r)+C_{r+1,4}\cosh(\lambda_2 x_r)=0 \tag{51}$$

$$\begin{aligned}&C_{r,1}\alpha_1\cos(\lambda_1 x_r)-C_{r,2}\alpha_1\sin(\lambda_1 x_r)+C_{r,3}\alpha_2\cosh(\lambda_2 x_r)+C_{r,4}\alpha_2\sinh(\lambda_2 x_r)\\&-C_{r+1,1}\alpha_1\cos(\lambda_1 x_r)+C_{r+1,2}\alpha_1\sin(\lambda_1 x_r)-C_{r+1,3}\alpha_2\cosh(\lambda_2 x_r)-C_{r+1,4}\alpha_2\sinh(\lambda_2 x_r)=0\end{aligned} \tag{52}$$

$$\begin{aligned}&-C_{r,1}\alpha_1\lambda_1\sin(\lambda_1 x_r)-C_{r,2}\alpha_1\lambda_1\cos(\lambda_1 x_r)+C_{r,3}\alpha_2\lambda_2\sinh(\lambda_2 x_r)+C_{r,4}\alpha_2\lambda_2\cosh(\lambda_2 x_r)\\&+C_{r+1,1}\alpha_1\lambda_1\sin(\lambda_1 x_r)+C_{r+1,2}\alpha_1\lambda_1\cos(\lambda_1 x_r)-C_{r+1,3}\alpha_2\lambda_2\sinh(\lambda_2 x_r)-C_{r+1,4}\alpha_2\lambda_2\cosh(\lambda_2 x_r)=0\end{aligned} \tag{53}$$

Writing Eqs. (50)–(53) in matrix form, one obtains

$$[B_r]\quad\{C_r\}=0 \tag{54}$$

where

$$\{C_r\}=\left\{\begin{array}{cccccccc}C_{r,1} & C_{r,2} & C_{r,3} & C_{r,4} & C_{r+1,1} & C_{r+1,2} & C_{r+1,3} & C_{r+1,4}\end{array}\right\} \tag{55}$$

and the coefficient matrix $[B_r]$ is given by Eq. (A.5) in Appendix A at the end of this paper.

If the left-end support of the beam is pinned as shown in Fig. 1, then the boundary conditions are

$$\overline{Y}_0(0)=\overline{\Psi'}_0(0)=0 \tag{56,57}$$

From Eqs. (16), (19) and (56), (57) one obtains

$$C_{0,2}+C_{0,4}=0 \tag{58}$$

$$-C_{0,2}\alpha_1\lambda_1+C_{0,4}\alpha_2\lambda_2=0 \tag{59}$$

or in matrix form

$$[B_0]\quad\{C_0\}=0 \tag{60}$$

where

$$[B_0]=\begin{array}{c}\begin{array}{cccc}1 & 2 & 3 & 4\end{array}\\\begin{bmatrix}0 & 1 & 0 & 1\\0 & -\alpha_1\lambda_1 & 0 & \alpha_2\lambda_2\end{bmatrix}\end{array}\begin{array}{c}1\\2\end{array} \tag{61}$$

$$\{C_0\}=\left\{\begin{array}{cccc}C_{0,1} & C_{0,2} & C_{0,3} & C_{0,4}\end{array}\right\} \tag{62}$$

If the right-end support of the beam is pinned as shown in Fig. 1, then the boundary conditions are

$$\overline{Y}_N(L)=\overline{\Psi'}_N(L)=0 \tag{63,64}$$

$$N=n+1 \tag{65}$$

From Eqs. (16), (19), (63) and (64), one obtains

$$C_{N,1}\sin(\lambda_1 L)+C_{N,2}\cos(\lambda_1 L)+C_{N,3}\sinh(\lambda_2 L)+C_{N,4}\cosh(\lambda_2 L)=0 \tag{66}$$

$$-C_{N,1}\alpha_1\lambda_1\sin(\lambda_1 L)-C_{N,2}\alpha_1\lambda_1\cos(\lambda_1 L)+C_{N,3}\alpha_2\lambda_2\sinh(\lambda_2 L)+C_{N,4}\alpha_2\lambda_2\cosh(\lambda_2 L)=0 \tag{67}$$

or in matrix form

$$[B_N]\quad\{C_N\}=0 \tag{68}$$

where

$$[B_N] = \begin{array}{c} \begin{array}{cccc} 4N-3 & 4N-2 & 4N-1 & 4N \end{array} \\ \left[\begin{array}{cccc} \sin(\lambda_1 L) & \cos(\lambda_1 L) & \sinh(\lambda_2 L) & \cosh(\lambda_2 L) \\ -\alpha_1\lambda_1 \sin(\lambda_1 L) & -\alpha_1\lambda_1 \cos(\lambda_1 L) & \alpha_2\lambda_2 \sinh(\lambda_2 L) & \alpha_2\lambda_2 \cosh(\lambda_2 L) \end{array}\right] \begin{array}{c} q-1 \\ q \end{array} \end{array} \tag{69}$$

$$\{C_N\} = \left\{ \begin{array}{cccc} C_{N,1} & C_{N,2} & C_{N,3} & C_{N,4} \end{array} \right\} \tag{70}$$

where q denotes the total number of equations for the integration constants given by

$$q = 4(\overline{v} + \overline{r}) + 5\overline{u} + 4 \tag{71}$$

From the next Eq. (72), one sees that the overall coefficient matrix $[\overline{B}]$ is a square matrix having q rows and q columns. Among the $q \times q$ coefficients of $[\overline{B}]$, $\overline{B}_{ab}$ ($a = 1, 2, \ldots, q$ and $b = 1, 2, \ldots, q$), the contribution of the sub-matrix $[B_0]$ given by Eq. (61) is given by $\overline{B}_{kl} = B_{0kl}$ with $k = 1, 2$ and $l = 1, 2, 3, 4$. In other words, digits 1, 2, 3 and 4 on top side of $[B_0]$ and those 1 and 2 on right-hand side of $[B_0]$ represent the identification numbers for the associated elements of the coefficient sub-matrix $[B_0]$ for achieving the overall coefficient matrix $[\overline{B}]$ by using the numerical assembly technique as done by the conventional finite element method (FEM). It is evident that, for the specified values of N and q, the digits determined by $4N-3$, $4N-2$, $4N-1$ and $4N$, shown on top side of $[B_N]$, and those determined by $q-1$ and q, shown on right-hand side of $[B_N]$, represent the identification numbers for the associated elements of the coefficient sub-matrix $[B_N]$.

4. Determination of natural frequencies and mode shapes of the beam

The integration constants relating to the left- and right-end supports of the beam are defined by Eqs. (62) and (70), respectively, while those relating to the intermediate stations are defined by Eqs. (35), (45) and/or (55) depending upon point mass, rotary inertia, linear spring, rotational spring, spring–mass system and/or rigid (pinned) support being located there. The associated coefficient matrices are given by $[B_0]$ (cf. Eq. (61)), $[B_u]$ (cf. Eq. (A.1) of Appendix A), $[B_v]$ (cf. Eq. (A.3) of Appendix A), $[B_r]$ (cf. Eq. (A.5) of Appendix A) and $[B_N]$ (cf. Eq. (69)). From the last equations concerned one may see that the identification numbers for each element of the last coefficient matrices are shown on the top side and right-hand side of each matrix. Therefore, using the numerical assembly technique as done by the conventional FEM one may obtain a matrix equation for all the integration constants of the entire beam

$$\left[\overline{B}\right]\left\{\overline{C}\right\} = 0 \tag{72}$$

Non-trivial solution of Eq. (72) requires that its coefficient determinant is equal to zero, i.e.,

$$\left|\overline{B}\right| = 0 \tag{73}$$

Which is the frequency equation for the present problem.

In this paper, the incremental search method is used to find the natural frequencies of the vibrating system, ω_i ($i = 1, 2, \ldots$). For each natural frequency ω_i, one may obtain the corresponding integration constants from Eq. (72). The substitution of the last integration constants into the displacement functions of the associated beam segments will determine the corresponding mode shape of the entire beam, $Y^{(i)}(X)$.

5. Numerical results and discussions

Before the free vibration analysis of a multispan Timoshenko beam carrying multiple concentrated elements is performed, the reliability of the theory and the computer program developed for this paper are confirmed by comparing the present results with those obtained from the conventional FEM. In FEM, the two-node beam elements are used and the entire beam is subdivided into 80 beam elements. Since each node has two degrees of freedom (dofs), the total dof for the entire unconstrained beam is 162. The dimensions of the Timoshenko beam studied in this paper are (cf. Fig. 1): the total length is $L = 1.0\,\mathrm{m}$; the mass density is

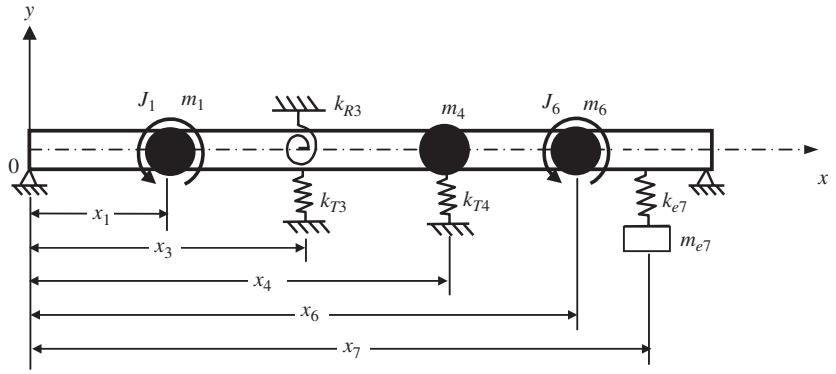

Fig. 2. Sketch for a pinned–pinned beam carrying three point masses, two rotary inertias, two linear springs, one rotational spring and one mass–spring system.

Table 1
The lowest five natural frequencies of the beam shown in Fig. 2 carrying three point masses, two rotary inertias, two linear springs, one rotational spring and one mass–spring system

Type of beam	Methods	Natural frequencies, ω_{Xi} (rad/s)				
		ω_{T1} or ω_{E1}	ω_{T2} or ω_{E2}	ω_{T3} or ω_{E3}	ω_{T4} or ω_{E4}	ω_{T5} or ω_{E5}
Type I						
Timoshenko beam	Present	343.5143	791.2395	2476.9018	4777.2470	6465.0813
	FEM	343.5144	791.2397	2476.9059	4777.2633	6465.1220
Euler–Bernoulli beam	Present	343.5574	794.4713	2535.9428	4957.8052	6751.0220
	[a](%)	(0.0125)	(0.4084)	(2.3837)	(3.7795)	(4.4228)
	FEM	343.5577	794.4716	2535.9430	4957.8055	6751.0235
Type II						
Timoshenko beam	Present	686.7688	1563.8251	4647.742	8663.0645	11614.2554
	FEM	686.7688	1563.8267	4647.7791	8663.2195	11614.5446
Euler–Bernoulli beam	Present	687.1147	1588.9425	5071.8856	9915.6103	13502.0439
	[a](%)	(0.0503)	(1.6062)	(9.1258)	(14.458)	(16.254)
	FEM	687.1154	1588.9433	5071.8860	9915.6110	13502.0473

[a](%) $= (\omega_{Ei}-\omega_{Ti})/\omega_{Ti} \times 100\%$.

$\rho = 7.835 \times 10^3\,\mathrm{kg/m^3}$ and Young's modulus is $E = 2.069 \times 10^{11}\,\mathrm{N/m^2}$, the shear coefficient is $k' = 5/6$, the Poisson ratio is $v = 0.3$, the shear modulus is $G = 7.9577 \times 10^{10}\,\mathrm{N/m^2}$.

5.1. A single-span Timoshenko beam carrying multiple concentrated elements

The first example is a pinned–pinned (P–P) beam as shown in Fig. 2 carrying three point masses, two rotary inertias, two linear springs, one rotational spring and one mass–spring system. Two types of cross-sections of the beam are investigated.

For Type I, the cross-sections of the beam is rectangular with width $b_{\mathrm{I}} = 0.05\,\mathrm{m}$ and height $h_{\mathrm{I}} = 0.06\,\mathrm{m}$. The distributions of the concentrated elements are: three point masses (m_1, m_4 and m_6) located at $x_1 = 0.2\,\mathrm{m}$, $x_4 = 0.6\,\mathrm{m}$ and $x_6 = 0.8\,\mathrm{m}$, respectively; two rotary inertias (J_1 and J_6) located at $x_1 = 0.2\,\mathrm{m}$ and $x_6 = 0.8\,\mathrm{m}$, respectively; two linear springs (k_{T3} and k_{T4}) located at $x_3 = 0.4\,\mathrm{m}$ and $x_4 = 0.6\,\mathrm{m}$, respectively; one rotational spring (k_{R3}) located at $x_3 = 0.4\,\mathrm{m}$ and one mass–spring system (with m_{e7} and k_{e7}) located at $x_7 = 0.9\,\mathrm{m}$. The corresponding parameters are: $m_1 = m_4 = 4.701\,\mathrm{kg}$, $m_6 = 9.402\,\mathrm{kg}$, $J_1 = 0.04701\,\mathrm{kg\,m^2}$, $J_6 = 0.14103\,\mathrm{kg\,m^2}$, $k_{T3} = 1.86210 \times 10^6\,\mathrm{N/m}$, $k_{T4} = 2.79315 \times 10^6\,\mathrm{N/m}$, $k_{R3} = 9.3105 \times 10^5\,\mathrm{N\,m}$, $m_{e7} = 4.701\,\mathrm{kg}$, $k_{e7} = 5.5863 \times 10^5\,\mathrm{N/m}$.

For Type II, the width of beam cross-sections is the same as that of Type I (i.e., $b_{II} = b_I = 0.05\,\text{m}$), but the depth is $h_{II} = 0.12\,\text{m}$. The distributions of the concentrated elements are also the same as Type I. The corresponding parameters are $m_1 = m_4 = 9.402\,\text{kg}$, $m_6 = 18.804\,\text{kg}$, $J_1 = 0.09402\,\text{kg m}^2$, $J_6 = 0.28206\,\text{kg m}^2$, $k_{T3} = 1.4897 \times 10^7\,\text{N/m}$, $k_{T4} = 2.2345 \times 10^7\,\text{N/m}$, $k_{R3} = 7.4484 \times 10^7\,\text{N m}$, $m_{e7} = 9.402\,\text{kg}$, $k_{e7} = 4.46904 \times 10^6\,\text{N/m}$. Table 1 shows the lowest five natural frequencies of the beam. In which, ω_{Ti} denotes the natural frequencies of the Timoshenko beam (with effects of shear deformation and rotary inertia considered), ω_{Ei} denotes the corresponding ones of the Euler–Bernoulli beam (with effects of shear deformation and rotary inertia neglected). It is seen that the current numerical results are in excellent agreement with those of FEM. In Table 1, the third line shows the percentage differences (%) between the lowest five natural frequencies of the Euler–Bernoulli beam and the corresponding ones of the Timoshenko beam for Type I, while the seventh line shows those for Type II. Because the main difference between beam Type I and beam Type II is in their depths and the larger the depth the higher the lowest five natural frequencies. This is the reason why the percentage differences (%) between the lowest five natural frequencies of the Euler–Bernoulli beam and the corresponding ones of the Timoshenko beam for Type II are greater than those for Type I.

It is noted that, for the present single-span example, the total number of intermediate stations is $n = 5$, including one intermediate spring–mass system (i.e., $\overline{u} = 1$), four intermediate concentrated elements (i.e., $\overline{v} = 4$) and no in-span support (i.e., $\overline{r} = 0$). Thus, according to Eq. (71), the total number of equations for the integration constants is $q = 4(\overline{v} + \overline{r}) + 5\overline{u} + 4 = 25$ In other words, the order of the overall coefficient matrix $[\overline{B}]$ is 25×25.

5.2. A multispan Timoshenko beam carrying multiple concentrated elements

The second example is a P–P beam with the distributions of concentrated elements and the corresponding parameters to be the same as of those of the first example but with one to two intermediate pinned supports. Cross-sections of Types I and II are investigated. Table 2 shows the lowest five natural frequencies of the beam with one intermediate pinned support located at $x_3 = 0.4$. Table 3 shows the lowest five natural frequencies of the beam with two intermediate pinned supports located at $x_3 = 0.4$ and $x_5 = 0.7$, respectively. From Tables 2 and 3, one sees that the current numerical results are in excellent agreement with those of FEM. Furthermore, the percentage differences between the lowest five natural frequencies of the Euler–Bernoulli beam and the corresponding ones of the Timoshenko beam increase with the increase of beam depth and span number. This is a reasonable result, because the lowest five natural frequencies of either the Euler–Bernoulli beam or the

Table 2
The lowest five natural frequencies of the *two-span* beam carrying three point masses, two rotary inertias, two linear springs, one rotational spring and one mass–spring system

Type of beam	Methods	Natural frequencies, ω_{Xi} (rad/s)				
		ω_{T1} or ω_{E1}	ω_{T2} or ω_{E2}	ω_{T3} or ω_{E3}	ω_{T4} or ω_{E4}	ω_{T5} or ω_{E5}
Type I						
Timoshenko beam	Present	344.0505	1630.4214	4666.1223	6410.2455	7724.3333
	FEM	344.0506	1630.4224	4666.1381	6410.2876	7724.4087
Euler–Bernoulli beam	Present	344.0948	1667.1936	4849.1637	6700.1525	8301.3915
	[a](%)	(0.0128)	(2.2554)	(3.9228)	(4.5226)	(7.4707)
	FEM	344.0950	1667.1943	4849.1649	6700.1530	8301.3921
Type II						
Timoshenko beam	Present	687.8352	3070.0901	8431.6168	11466.2293	12962.8693
	FEM	687.8353	3070.0988	8431.7648	11466.5627	12963.4151
Euler–Bernoulli beam	Present	688.1895	3334.3872	9698.3274	13400.3049	16602.7830
	[a](%)	(0.0515)	(8.6088)	(15.0230)	(16.8680)	(28.0800)
	FEM	688.1900	3334.3887	9698.3299	13400.3062	16602.7846

[a](%) $= (\omega_{Ei} - \omega_{Ti})/\omega_{Ti} \times 100\%$.

Table 3
The lowest five natural frequencies of the *three-span* beam carrying three point masses, two rotary inertias, two linear springs, one rotational spring and one mass–spring system

Type of beam	Methods	Natural frequencies, ω_{Xi} (rad/s)				
		ω_{T1} or ω_{E1}	ω_{T2} or ω_{E2}	ω_{T3} or ω_{E3}	ω_{T4} or ω_{E4}	ω_{T5} or ω_{E5}
Type I						
Timoshenko beam	Present	344.5052	4661.1268	6201.4770	7724.1679	9780.4794
	FEM	344.5053	4661.1421	6201.5263	7724.2427	9780.6085
Euler–Bernoulli beam	Present	344.5391	4844.6172	6496.8886	8299.6140	12301.4300
	[a](%)	(0.0098)	(3.9366)	(4.7636)	(7.4499)	(25.7750)
	FEM	344.5394	4844.6175	6496.8901	8299.6153	12301.4306
Type II						
Timoshenko beam	Present	688.8075	8417.9381	10967.4659	12929.3475	13490.0384
	FEM	688.8076	8418.0796	10967.9022	12929.7347	13490.6182
Euler–Bernoulli beam	Present	689.0781	9689.23447	12993.7772	16599.2279	24602.8599
	[a](%)	(0.0392)	(15.1022)	(18.4756)	(28.38411)	(82.3779)
	FEM	689.0788	9689.2351	12993.7805	16599.2311	24602.8627

[a](%) $= (\omega_{Ei}-\omega_{Ti})/\omega_{Ti} \times 100\%$.

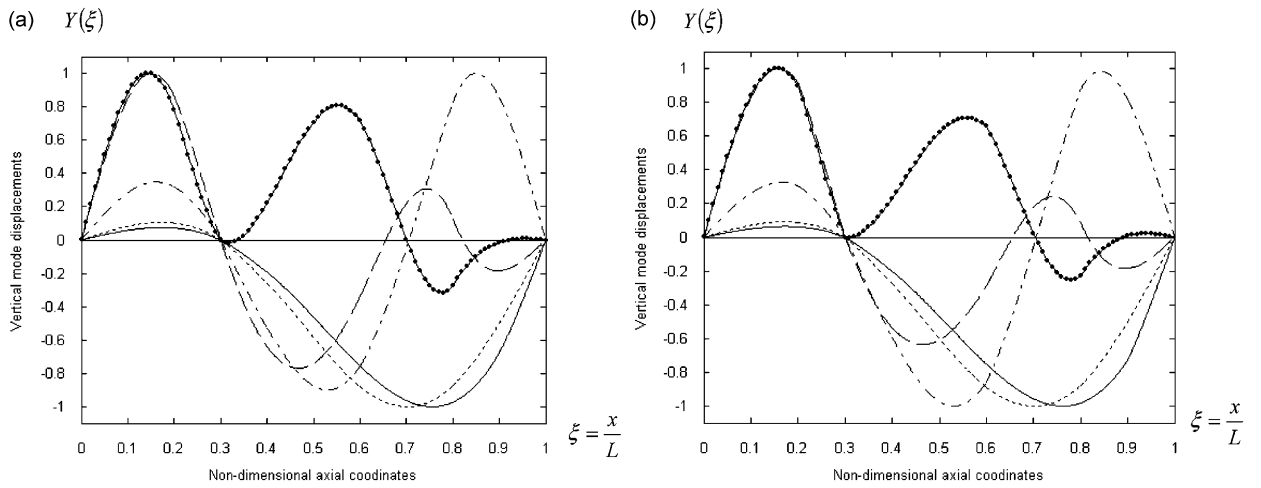

Fig. 3. The lowest five mode shapes of the *two-span* pinned–pinned (P–P) Timoshenko beam carrying three point masses, two rotary inertias, two linear springs, one rotational spring and one mass–spring system for (a) Type I beam and (b) Type II beam.

Timoshenko beam increase with the increase of beam depth and span number, and the effects of shear deformation and rotary inertia increase with the increase of the lowest five natural frequencies of the beam. Fig. 3 shows the lowest five mode shapes of the two-span P–P Timoshenko beam with the first, second, third, fourth and fifth mode shapes represented by the curves ——, ·····, – – – –, – – –, and –·–·–, respectively, in which Fig. 3(a) is for Type I beam and Fig. 3(b) is for Type II beam. Fig. 4 shows the lowest five mode shapes of the three-span P–P Timoshenko beam with the first, second, third, fourth and fifth mode shapes represented by the curves ——, ·····, – – – –, – – –, and –·–·–, respectively, for (a) Type I beam and (b) Type II beam.

For the current example with "two spans," the total number of intermediate stations is $n = 6$, including one intermediate spring–mass system (i.e., $\overline{u} = 1$), four intermediate concentrated elements (i.e., $\overline{v} = 4$) and one in-span support (i.e., $\overline{r} = 1$). Thus, the total number of equations for the integration constants is $q = 4(\overline{v}+\overline{r}) + 5\overline{u} + 4 = 29$ and the order of the overall coefficient matrix $[\overline{B}]$ is 29×29. It is evident that the order of the overall coefficient matrix $[\overline{B}]$ is 33×33 for the "three-span" case, because four more equations must be considered due to one more in-span support.

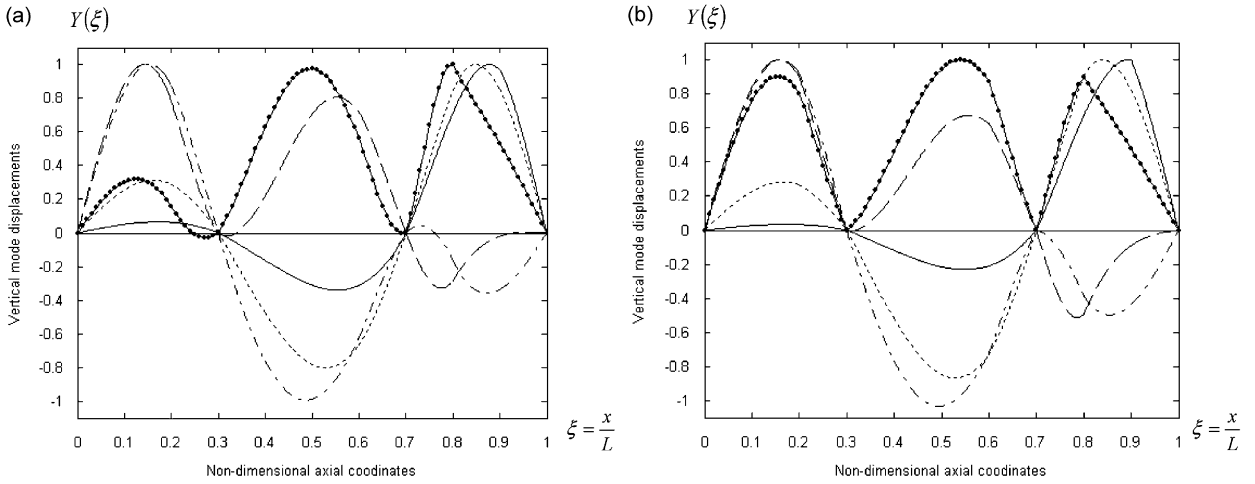

Fig. 4. The lowest five mode shapes of the *three-span* pinned–pinned (P–P) Timoshenko beam carrying three point masses, two rotary inertias, two linear springs, one rotational spring and one mass–spring system for (a) Type I beam and (b) Type II beam.

6. Conclusions

Because the literature regarding the "exact" solutions for the natural frequencies and associated mode shapes of a multispan Timoshenko beam carrying multiple concentrated elements (such as point masses with rotary inertias, linear springs, rotational springs and/or spring–mass systems) are rare, and the classical analytical methods will suffer much difficulty for the last problem, the theory and "exact" solutions by using the numerical assembly method (NAM) for the examples presented in this paper will be useful for checking the accuracy of the numerical results obtained from various "approximate" methods.

Appendix A

$$[B_u] = \begin{array}{c} \begin{matrix} 4u-3 & 4u-2 & 4u-1 & 4u & 4u+1 & 4u+2 & 4u+3 & 4u+4 & 4u+5 \end{matrix} \\ \begin{bmatrix} \mathrm{s}\theta_{u1} & \mathrm{c}\theta_{u1} & \mathrm{sh}\theta_{u2} & ch\theta_{u2} & -\mathrm{s}\theta_{u1} & -\mathrm{c}\theta_{u1} & -\mathrm{sh}\theta_{u2} & -ch\theta_{u2} & 0 \\ \alpha_1 \mathrm{c}\theta_{u1} & -\alpha_1 \mathrm{s}\theta_{u1} & \alpha_2 ch\theta_{u2} & \alpha_2 \mathrm{sh}\theta_{u2} & -\alpha_1 \mathrm{c}\theta_{u1} & \alpha_1 \mathrm{s}\theta_{u1} & -\alpha_2 ch\theta_{u2} & -\alpha_2 \mathrm{sh}\theta_{u2} & 0 \\ -\alpha_1\lambda_1 \mathrm{s}\theta_{u1} & -\alpha_1\lambda_1 \mathrm{c}\theta_{u1} & \alpha_2\lambda_2 \mathrm{sh}\theta_{u2} & \alpha_2\lambda_2 ch\theta_{u2} & \alpha_1\lambda_1 \mathrm{s}\theta_{u1} & \alpha_1\lambda_1 \mathrm{c}\theta_{u1} & -\alpha_2\lambda_2 \mathrm{sh}\theta_{u2} & -\alpha_2\lambda_2 ch\theta_{u2} & 0 \\ \varepsilon_1 \mathrm{c}\theta_{u1} + F_u^* \mathrm{s}\theta_{u1} & -\varepsilon_1 \mathrm{s}\theta_{u1} + F_u^* \mathrm{c}\theta_{u1} & \varepsilon_2 ch\theta_{u2} + F_u^* \mathrm{sh}\theta_{u2} & \varepsilon_2 \mathrm{sh}\theta_{u2} + F_u^* ch\theta_{u2} & -\varepsilon_1 \mathrm{c}\theta_{u1} & +\varepsilon_1 \mathrm{s}\theta_{u1} & -\varepsilon_2 ch\theta_{u2} & -\varepsilon_2 \mathrm{sh}\theta_{u2} & 0 \\ \mathrm{s}\theta_{u1} & \mathrm{c}\theta_{u1} & \mathrm{sh}\theta_{u2} & ch\theta_{u2} & 0 & 0 & 0 & 0 & \sigma_u^2 - 1 \end{bmatrix} \end{array} \begin{matrix} \\ 4u-2 \\ 4u-1 \\ 4u \\ 4u+1 \\ 4u+2 \end{matrix} \tag{A.1}$$

$$\theta_{u1} = \lambda_1 x_u, \quad \theta_{u2} = \lambda_2 x_u, \quad s\theta_{u1} = \sin\theta_{u1}, \quad c\theta_{u1} = \cos\theta_{u1}, \quad sh\theta_{u2} = \sinh\theta_{u2}, \quad ch\theta_{u2} = \cosh\theta_{u2}$$
$$\alpha_1 = \frac{\lambda_1}{[1-(J\bar{\omega}^2/k'AG)] + (EI/k'AG)\lambda_1^2}, \quad \alpha_2 = \frac{\lambda_2}{[1-(J\bar{\omega}^2/k'AG)] - (EI/k'AG)\lambda_2^2}, \quad F_u^* = \frac{m_{\mathrm{eu}}\omega^2}{1-(\omega/\omega_{eu})^2}$$
$$\varepsilon_1 = k'AG(\alpha_1 - \lambda_1), \quad \varepsilon_2 = k'AG(\alpha_2 - \lambda_2), \quad \sigma_u = (\omega/\omega_{eu})^2 - 1 \tag{A.2}$$

$$[B_v] = \begin{array}{c} \begin{matrix} 4v-3 & 4v-2 & 4v-1 & 4v & 4v+1 & 4v+2 & 4v+3 & 4v+4 \end{matrix} \\ \begin{bmatrix} s\theta_{v1} & c\theta_{v1} & sh\theta_{v2} & ch\theta_{v2} & -s\theta_{v1} & -c\theta_{v1} & -sh\theta_{v2} & -ch\theta_{v2} \\ \alpha_1 c\theta_{v1} & -\alpha_1 s\theta_{v1} & \alpha_2 ch\theta_{v2} & \alpha_2 sh\theta_{v2} & -\alpha_1 c\theta_{v1} & \alpha_1 s\theta_{v1} & -\alpha_2 ch\theta_{v2} & -\alpha_2 sh\theta_{v2} \\ -\beta_1 s\theta_{v1} + \phi_1 c\theta_{v1} & -\beta_1 c\theta_{v1} - \phi_1 s\theta_{v1} & \beta_2 sh\theta_{v2} + \phi_2 ch\theta_{v2} & \beta_2 ch\theta_{v2} + \phi_2 sh\theta_{v2} & \beta_1 s\theta_{v1} & \beta_1 c\theta_{v1} & -\beta_2 sh\theta_{v2} & -\beta_2 ch\theta_{v2} \\ \eta_1 s\theta_{v1} + \varepsilon_1 c\theta_{v1} & \eta_1 c\theta_{v1} - \varepsilon_1 s\theta_{v1} & \eta_1 sh\theta_{v2} + \varepsilon_2 ch\theta_{v2} & \eta_1 ch\theta_{v2} + \varepsilon_2 sh\theta_{v2} & -\varepsilon_1 c\theta_{v1} & \varepsilon_1 s\theta_{v1} & -\varepsilon_2 ch\theta_{v2} & -\varepsilon_2 sh\theta_{v2} \end{bmatrix} \end{array} \begin{matrix} \\ 4v-1 \\ 4v \\ 4v+1 \\ 4v+2 \end{matrix} \tag{A.3}$$

$$\theta_{v1}=\lambda_1 x_v,\quad \theta_{v2}=\lambda_2 x_v,\quad s\theta_{v1}=\sin\theta_{v1},\quad c\theta_{v1}=\cos\theta_{v1},\quad sh\theta_{v2}=\sinh\theta_{v2},\quad ch\theta_{v2}=\cosh\theta_{v2}$$
$$\beta_1=EI\alpha_1\lambda_{11},\quad \beta_2=EI\alpha_2\lambda_2,\quad \phi_1=\alpha_1(k_{Rv}-J_v\omega^2),\quad \phi_2=\alpha_2(k_{Rv}-J_v\omega^2),$$
$$\eta_1=(m_v\omega^2-k_{Tv})\quad \varepsilon_1=k'AG(\alpha_1-\lambda_1)\quad \varepsilon_2=k'AG(\alpha_2-\lambda_2) \tag{A.4}$$

$$[B_r]=\begin{array}{c} \begin{matrix} 4r-3 & 4r-2 & 4r-1 & 4r & 4r+1 & 4r+2 & 4r+3 & 4r+4 \end{matrix} \\ \begin{bmatrix} s\theta_{r1} & c\theta_{r1} & sh\theta_{r2} & ch\theta_{r2} & 0 & 0 & 0 & 0 \\ 0 & 0 & 0 & 0 & s\theta_{r1} & c\theta_{r1} & sh\theta_{r2} & ch\theta_{r2} \\ \alpha_1 c\theta_{r1} & -\alpha_1 s\theta_{r1} & \alpha_2 ch\theta_{r2} & \alpha_2 sh\theta_{r2} & -\alpha_1 c\theta_{r1} & \alpha_1 s\theta_{r1} & -\alpha_2 ch\theta_{r2} & -\alpha_2 sh\theta_{r2} \\ -\alpha_1\lambda_1 s\theta_{r1} & -\alpha_1\lambda_1 c\theta_{r1} & \alpha_2\lambda_2 s\theta_{r2} & \alpha_2\lambda_2 ch\theta_{r2} & \alpha_1\lambda_1 s\theta_{r1} & \alpha_1\lambda_1 c\theta_{r1} & -\alpha_2\lambda_2 sh\theta_{r2} & -\alpha_2\lambda_2 ch\theta_{r2} \end{bmatrix} \end{array} \begin{matrix} 4r-1 \\ 4r \\ 4r+1 \\ 4r+2 \end{matrix} \tag{A.5}$$

$$\theta_{r1}=\lambda_1 x_r,\quad \theta_{r2}=\lambda_2 x_r,\quad s\theta_{r1}=\sin\theta_{r1},\quad c\theta_{r1}=\cos\theta_{r1},\quad sh\theta_{r2}=\sinh\theta_{r2},\quad ch\theta_{r2}=\cosh\theta_{r2}$$

References

[1] J.C. Bruch Jr., T.P. Mitchell, Vibrations of a mass-loaded clamped–free Timoshenko beam, *Journal of Sound and Vibration* 114 (1987) 341–345.

[2] W.H. Liu, D.S. Liu, Natural frequencies of a restrained Timoshenko beam with a tip body at its free end, *Journal of Sound and Vibration* 128 (1989) 167–173.

[3] H. Abramovich, I. Elishakoff, Influence of shear deformation and rotary inertia on vibration frequencies via Loves equation, *Journal of Sound and Vibration* 137 (1990) 516–522.

[4] H. Abramovich, I. Elishakoff, Vibration of a cantilever Timoshenko beam with a tip mass, *Journal of Sound and Vibration* 148 (1991) 162–170.

[5] M.J. Maurizi, M. Bellés, Natural frequencies of the beam–mass system: comparison of the two fundamental theories of beam vibration, *Journal of Sound and Vibration* 150 (1991) 330–334.

[6] H. Abramovich, O. Hamburger, Vibration of a uniform cantilever Timoshenko beam with translational and rotational springs and with a tip mass, *Journal of Sound and Vibration* 154 (1992) 67–80.

[7] R.E. Rossi, P.A.A. Laura, D.R. Avalos, H. Larrondo, Free vibration of Timoshenko beams carrying elastically mounted, concentrated masses, *Journal of Sound and Vibration* 165 (1993) 209–223.

[8] B. Posiadala, Free vibrations of uniform Timoshenko beams with attachments, *Journal of Sound and Vibration* 204 (1997) 359–369.

[9] S.W. Hong, J.W. Kim, Modal analysis of multi-span Timoshenko beams connected or supported by resilient joints with damping, *Journal of Sound and Vibration* 227 (1999) 787–806.

[10] M. Gürgöze, On the eigenfrequencies of a cantilever beam with attached tip mass and a spring–mass system, *Journal of Sound and Vibration* 190 (1996) 149–162.

[11] M. Gürgöze, On the alternative formulation of the frequency equation of a Bernoulli–Euler beam to which several spring–mass systems are attached in-span, *Journal of Sound and Vibration* 217 (1998) 585–595.

[12] M. Gürgöze, H. Erol, Determination of the frequency response function of a cantilever beam simply supported in-span, *Journal of Sound and Vibration* 247 (2001) 351–367.

[13] J.S. Wu, D.W. Chen, Free vibration analysis of a Timoshenko beam carrying multiple spring–mass systems by using he numerical assembly technique, *International Journal for Numerical Methods in Engineering* 50 (2001) 1039–1058.

[14] J.S. Wu, C.T. Chen, A lumped-mass TMM for free vibration analysis of a multi-step Timoshenko beam carrying eccentric lumped masses with rotary inertias, *Journal of Sound and Vibration* 301 (2007) 878–897.

[15] H.Y. Lin, Y.C. Tsai, Free vibration analysis of a uniform multi-span beam carrying multiple spring–mass systems, *Journal of Sound and Vibration* 302 (2007) 442–456.

[16] H.Y. Lin, Y.C. Tsai, On the natural frequencies and mode shapes of a multiple-step beam carrying a number of intermediate lumped masses and rotary inertias, *Structural Engineering and Mechanics* 22 (2006) 701–717.

[17] S.P. Timoshenko, *Vibration Problems in Engineering*, third ed., D. Van Nostrand Company, New York, 1955.